Hindawi
Advances in Civil Engineering
Volume 2022, Article ID 9946957, 13 pages
https://doi.org/10.1155/2022/9946957

Research Article

Study on the Technical Status of Old Concrete Truss-Arch Bridge Based on Vehicle-Bridge Interaction

Renchao Xie, Ming Li, and Chihao Xu

College of Civil Engineering, Suzhou University of Science and Technology, Suzhou 215000, China

Correspondence should be addressed to Ming Li; liming@usts.edu.cn

Received 10 March 2022; Revised 3 September 2022; Accepted 14 September 2022; Published 19 October 2022

Academic Editor: Pengfei Liu

With the rapid development of the country's economy, a large number of heavy vehicles are being used due to the expansion of transportation demand and increased transportation costs. For the old concrete truss-arch bridges built in the last century, the bridges may hardly meet the modern traffic volume. With respect to old bridges in poor condition, it takes more time and resources to evaluate the technical status by field load tests, and there are some safety risks. A finite element method based on vehicle-bridge coupled vibration theory was proposed for evaluating the technical status of concrete truss-arch bridges in this paper. An old concrete truss-arch bridge in the suburbs of Suzhou, China, was selected as the research object. The field static and dynamic load tests were conducted and the results are consistent with the results of the numerical simulation based on the method proposed in this study. It can be concluded that the proposed numerical method can be widely used to assess the technical state of the old concrete truss-arch bridges in poor condition.

1. Introduction

On August 24, 2012, an appalling accident occurred in Harbin. The collapse of the bridge caused numerous deaths and injuries, as illustrated in Figure 1. On October 10, 2020, National Highway 312 in Jiangsu Province collapsed due to heavy vehicles, as illustrated in Figure 2. Bridge collapse accidents have occurred in many countries in recent years, and most of these accidents were caused by the lack of maintenance of aging bridges. According to incomplete statistics, thousands of bridge collapse accidents have occurred in this century, causing tens of thousands of casualties. Nearly half of the small and medium-span concrete bridges in our country were built from the 1950s to the 1980s, and most of them were in "disease-carrying" condition, which made it difficult to meet modern traffic levels according to past design norms. Bridges have lagged behind as infrastructure and have become a "feature" of the last century. The bridge structure will be damaged to a certain extent under the long-term load of heavy vehicles. Especially for old bridges with medium and small spans, the vibration of bridges under the action of heavy vehicles is becoming more and more obvious. Therefore, a systematic technical status assessment is needed for the aging concrete bridges with small and medium spans. Technical status assessment refers to a comprehensive on-site inspection of the existing status of severely damaged and old bridges, detection of various parameters of bridge components, identification of bridge damage and development trends, and systematic assessment of the carrying capacity of old bridges to determine whether the current carrying capacity of bridges meets the needs of traffic, providing a technical basis and recommendations for bridge maintenance and repair.

The dynamic response characteristics of bridges are usually expressed using impact factors, which are comprehensive coefficients influenced by a number of important factors and can reflect the impact of heavy vehicles on bridges. The deflection and strain under heavy vehicles are usually tested in the field load experiments and the ratio of dynamic deflection to corresponding static deflection is the impact factor. It is often determined by national codes using a single parametric formula through a large amount of test data, making it difficult to fully reflect the actual vibration conditions of different types of bridges. The bridge design

Figure 1: Collapse of the YangMingTan bridge.

Figure 2: Rollover of viaduct in WuXi.

code takes the fundamental frequency of the bridge as the parameter in China [1]. Li Yuliang of Jilin Institute of Transportation Science collected more than 6,600 impact coefficient sample data from seven bridges of different spans and collated them to obtain the relationship equation between bridge frequency and impact factor, which was adopted by the revision of China's General Specification for Highway Bridge and Culvert Design (JTG D60-2015) [1]. The relationship between bridge span and impact factor is generally inversely proportional in bridge design codes such as in Japan and the United States.

In general, field load testing is an effective method to investigate the fundamental behavior and establish the essential data of bridges. For most researchers, it is an effective method that the aging bridge can be achieved through field load tests to assess the capacity of the damaged and deteriorated portions of the bridge. This method can overcome the problem of the material properties, field conditions, and uncertainties in the present situation partially. The field load tests can be used for bridge load rating [2], the strength of components [3], and bridge performance [4]. Nondestructive field testing has been used in the past to better understand the behavior of steel girder bridges [5]; Tevfik Terzioglu tested the spread slab beam bridge to evaluate constructability and structural performance under static and dynamic vehicular loads [6]; the longest cable-stayed bridge in Taiwan was selected with 40 loading cases to investigate the bridge's behavior by field load test [7].

However, most old bridges need to be repaired and continue to serve with the disease, while dynamic and static load tests require a lot of time and money to ensure the safety of the bridge in the long term. Even for some old concrete bridges with serious damage, if the field load test is carried out directly, it will affect the safety of the bridge. Therefore, we need a safe and effective method that can quickly and systematically evaluate the technical status of many old bridges. Finite element simulation has been proposed to measure the dynamic response characteristics of bridges quickly. The expression of impact factor was proposed for small and medium-span aged bridges with poor road surface conditions [8]. Deng Lu studied on dynamic impact factors of simply-supported prestressed concrete girder bridges under vehicle braking [9] and the IF(impact factor) of shear force and bending moment of simply-supported and continuous bridges were studied [10]. Nan Zhang used the pseudoexcitation method to evaluate the safety of the simply-supported girder bridge under a high-speed train based on vehicle-bridge interaction [11]. Dynamic response of viscoelastic asphalt pavement under vehicle-bridge interaction load was studied [12]. Some scholars consider the service performance of bridges from fatigue damage and damage detection for ageing bridges. A simultaneous identification method for identifying bridge damage and vehicle parameters is proposed [13]. The life of an ageing prestressed concrete bridge under fatigue damage is estimated by numerical simulation [14].

The maintenance of old bridges is always ignored in most countries because of a lack of related drawings and data that make maintenance difficult to complete. Safety evaluation is of great significance for aged bridges and has attracted extensive attention in recent years. However, few scholars have studied the carrying capacity of old bridges with disease, and most of the relevant specifications are based on empirical formulas that make it difficult to accurately assess the real situation of bridges. Filed load tests are mostly used in this field of old bridges, and it is unsustainable that dynamic and static load tests require a lot of time and money to ensure the safety of the bridge in the long term. At this stage, hundreds of thousands of old concrete bridges in China need to be urgently analyzed by the finite element method to ensure their safety and continue to serve with the disease. Therefore, considering the condition of bridge damage, the technical status of the old concrete truss-arch bridges was systematically evaluated using the vehicle-bridge interaction theory in this article.

More than 300 old concrete bridges in the suburbs of Suzhou in China were selected for on-site damage detection. Compared with other types of bridges such as concrete slab bridges and concrete beam bridges, concrete truss-arch bridges were selected because of their special structural forms. A large number of cracks have been generated under the action of long-term heavy vehicles. At the same time, there are few studies on truss-arch bridges in the field of vehicle-bridge interaction. A concrete truss-arch bridge with serious damage and many cracks was studied in this article.

Field detection was carried out to preliminarily evaluate the old bridges and imported important parameters (such as component damage, cracks, and roughness of the road surface) into the finite element analysis. The technical status

of the old bridges was evaluated through the change value of the impact factor and the limit value of the relevant bridge specifications. Finally, the field load test will be compared with the results obtained by this method to verify the accuracy of the finite element simulation. This method can provide a theoretical basis for the maintenance and management of many old bridges accurately and quickly and has important engineering significance.

2. Algorithms of Vehicle-Bridge Interaction

Numerical investigations have been conducted on the vehicle-bridge interaction problem by many researchers. Wang [15] and Harris [16] contributed to the improved modelling of vehicles. Three-axle vehicles and five-axle vehicles were proposed according to the American bridge design codes and European vehicle model statistics. The proposed theory is classical by Huang and Wang. The cable stayed bridge considering the road surface roughness is a classic impact analysis for Huang and Wang [17]. The theoretical development research is sorted out, and the impact factor was proposed by Deng [18] for vehicle-bridge interactions. Zhen Sun [19] presented a practical and efficient iterative method for predicting the vehicle-induced response of bridges. Milan Sokol presented the SHM (structural health monitoring) to use static and dynamic load tests to confirm the load-bearing capacity of the bridge with numerical simulations [20]. Lu Zhang proposed the dynamic vibration property of the vehicle-bridge expansion joint coupled system with the proposed model [21].

The complex vehicle-bridge interaction can be explained by the following formula [22], and these equations can also be expressed by a matrix.

$$\begin{aligned} f(t) &= F\left(v(t), b\left(x_c(t), t\right), r\left(x_c(t)\right), g\right), \\ V(v(t)) &= f(t), \\ B(bx, t) &= \delta x_c(t) f(t), \end{aligned} \tag{1}$$

where $f(t)$ is the contact force between the wheel and the bridge deck at time t, which can be expressed by vehicle speed v, response function b, road surface roughness r, and gravity acceleration g. Functions V and B represent the two independent subsystems of the vehicle and bridge, respectively. In the calculation process, the whole vehicle-bridge system is divided into two independent subsystems, and the vehicle modelled by MATLAB is imported into the bridge in ABAQUS for finite element analysis.

3. Field Test

3.1. Bridge Description. The term "truss-arch bridge" means that the two sides of the arch circle support the superstructure with truss members, and the two parts of the arch circle are combined with a deck plate and transverse connection system. The truss member mainly bears the axial force of the truss-arch bridge, and the arch ring has enough horizontal thrust to reduce the midspan bending moment of the bridge, so the truss-arch bridge has the advantages of both truss and arch bridges. The truss-arch bridge can give full play to the material properties of the full section of each component, save more material than other girder bridges of the same span, has the characteristics of integrity, light mass, good structural forces, etc., and can be built on soft soil foundations. Therefore, truss-arch bridges with medium and small spans were widely built in the last century. Since the truss-arch bridge structure is more complex and the truss rods are more slender and mostly made of reinforced concrete, cracks are prone to occur at some bridge tension, bending, and rigid nodes under long-term vehicle action.

Figure 3: Frontage view of the bridge.

Figure 4: Side view of the bridge.

The Zhihong Bridge in Taicang City was selected as the research object. There are large production workshops around the bridge that are often affected by heavy vehicles, and the damage to components is serious. When heavy vehicles pass the bridge, the bridge vibrates violently, and there is no load limit sign on either side of the bridge, which will cause the bridge to be very dangerous. The truss-arch bridge is a 41 m single-span bridge with a width of 7.0 m. The thickness of the deck is 0.2 m, and the concrete cover is 35 mm. The reinforced concrete deck is supported by truss girders. The superstructure is truss-arch, and the supporting structure is a mortar block stone gravity abutment with a shallow foundation, as illustrated in Figure 3 and 4.

3.2. Field Measure for Bridge Damage. We detected a comprehensive field measurement of various components of the bridge. Although bridges were built in the last century without accurate data, we need to identify the defects and severity of components to evaluate their impact on the bearing capacity of bridges. Technical evaluation can be conducted according to bridge components, superstructure, bearer, and pavement through field investigation, adopting

(a) (b)

(c) (d)

Figure 5: Different parts of the bridge damage. (a) Breakage expansion joint. (b) Bridge surface fracture. (c) Exposed reinforcing bar of truss beam. (d) Abutment crack.

hierarchical comprehensive evaluation of bridge control indicators and then conducting overall evaluation. According to the experience of engineers, the current use safety of bridges is preliminarily judged.

The bridge deck had varying degrees of abrasion, and the components of the bridge were damaged. The strength of concrete was approximately 52.8~53.8 MPa by the ultrasonic rebound method. The ratio of the characteristic value of the protective layer thickness of the concrete structure to the design value was between 1.22 and 1.25, and the influence of the protective layer durability of the structural reinforcement was not obvious. However, the carbonation depth of concrete is relatively large if the continuous development will cause damage to the passive film on the surface of steel bars, resulting in gradual corrosion of steel bars and reducing the bearing capacity of bridges. The damage is shown in Figure 5 for parts of the bridge. The preliminary professional evaluation of Zhihong Bridge was carried out, and the main components of the bridge have large defects, which affect the function of the bridge.

These tests are to obtain more accurate information about bridges. Bridge detection is essential for older bridges (specialized agencies conduct tests at one to three month intervals in many regions) and needs to be carried out on a long-term basis to prevent the sudden expansion of previous cracks or the appearance of new cracks on bridges. The strength and stiffness of components are difficult to achieve within the design parameters of drawings for ageing bridges. Conventional bridge inspection can adjust the information of design drawings and even the bridge data are provided for bridges without drawings.

3.3. Test Vehicle. There are two means of investigating the complicated bridge-vehicle interaction problem as follows: experimental and analytical approaches. We investigated some passing heavy vehicles, of which most of them were three-axle heavy vehicles with a load limit of 35 tons made in China, which is commonly chosen in the experiment. The vehicle model was taken as that used by Kim [23] and was simulated with a realistic 3D vehicle model (bilateral symmetry) that could represent the design vehicle load and actual vehicle dynamic characteristics. We calibrated the vehicle precisely. The model assumes that the body is rigid, consisting of three mass blocks and connecting rods with eight degrees of freedom, and that wheels are connected to the ground by damping springs, as illustrated in Figure 6.

3.4. Static Load Test. The traditional field load test requires that the deflection and strain of the bridges do not exceed the specification requirements and analyzes the value of

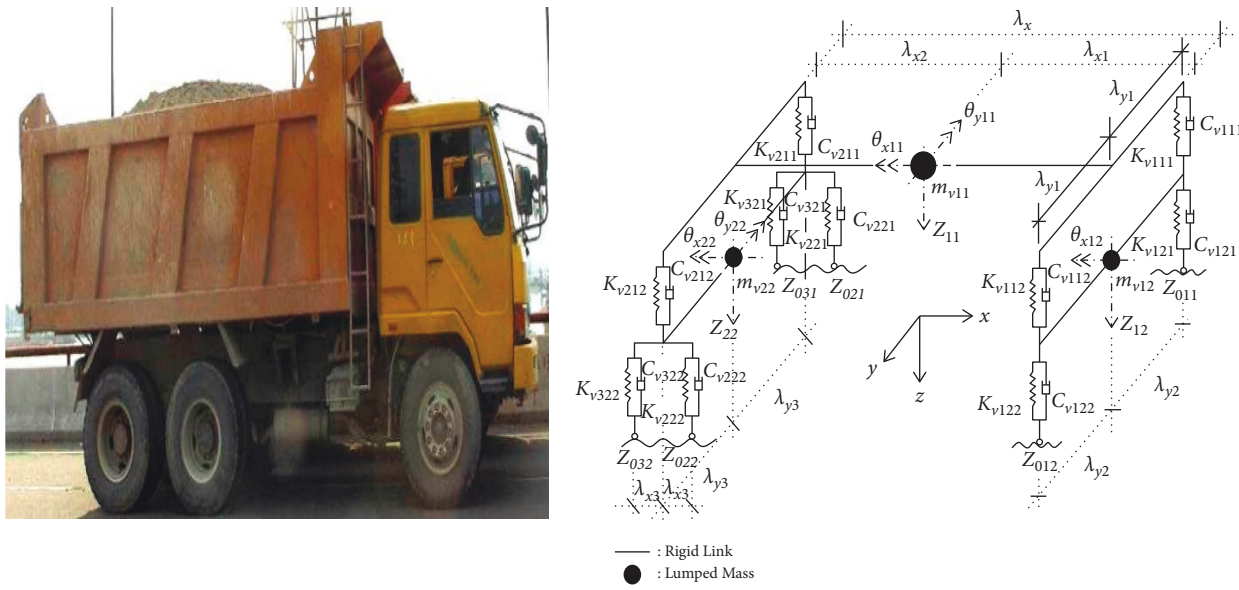

Figure 6: Heavy vehicle model. (a) Test heavy vehicle. (b) Three-axle vehicle with eight degrees of freedom.

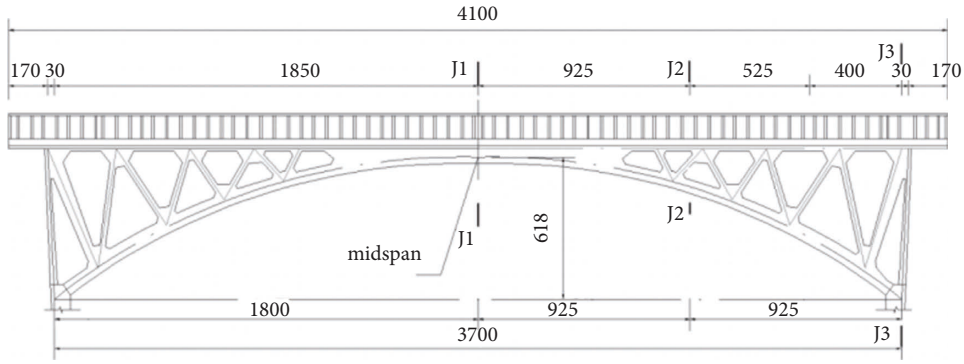

Figure 7: Position chart of the control section.

the impact factor to determine the structural performance of bridges. According to the Chinese norm "load test methods for highway bridges," the unfavourable positions of the structure of the section layout were selected. The static load test selected the mid-span, a-quarter-span, and arch springing to set the strain gauge. The numbers were J1, J2, and J3, respectively, and four strain gauges were set at the bottom of the bridge deck. As illustrated in Figures 7 and 8, the internal force equivalent principle was chosen to grade the load, which was divided into three loading levels. First, a heavy vehicle traveled to the present position to measure the strain and deflection of the bridge deck. Then, another heavy vehicle was parallel to it and remained stationary for secondary loading. Two heavy vehicles left the bridge to measure the residual strain. The loading test took no more than 20 minutes per cycle [24], as illustrated in Figure 9.

In the process of the test, the implementation of loading should be unified and commanded by professionals to grasp all aspects in time. It is necessary to ensure the safety of the

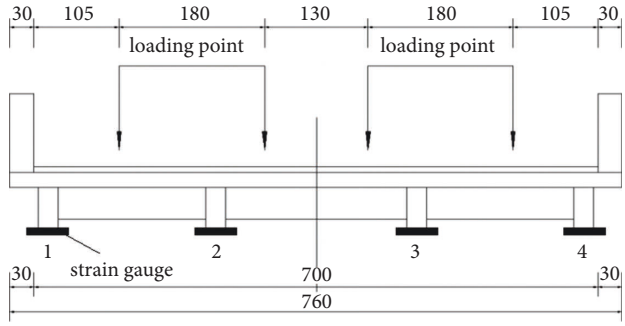

Figure 8: Loading profile.

structure and personnel; meanwhile, we should observe whether the strain and deflection of the bridge exceed the theoretical value. The static load test results are shown in Tables 1 and 2.

The strain value exceeds the theoretical value at the middle span of the bridge under a heavy vehicle load, indicating that the actual working state of the test section is

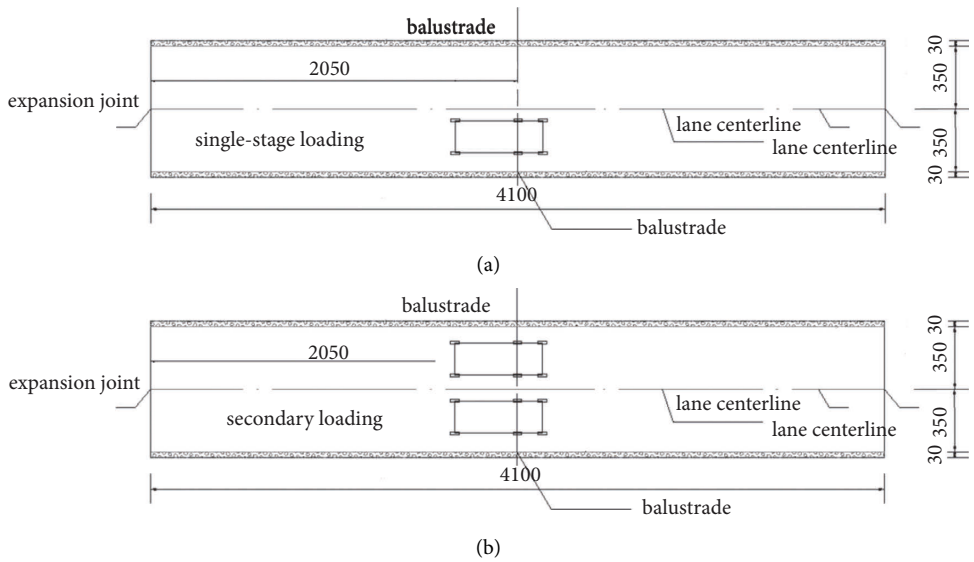

Figure 9: Steps of the static load test. (a) Single-stage loading. (b) Secondary loading.

Table 1: Theory and experimental strain values.

Number of measuring points	Single-stage loading	Secondary loading		Unloading
	Experimental value ($\mu\varepsilon$)	Experimental value ($\mu\varepsilon$)	Theoretical value ($\mu\varepsilon$)	Residual strain ($\mu\varepsilon$)
J1-1	21	40	30	0
J1-2	49	102	80	0
J1-3	30	84	80	1
J1-4	15	30	30	0
J2-1	13	21	27	0
J2-2	24	61	83	0
J2-3	30	70	87	0
J2-4	19	24	30	0
J3-1	20	48	30	0
J3-2	18	41	35	0
J3-3	20	42	35	0
J3-4	25	38	30	0

Table 2: Theory and experimental displacement values.

Position	Single-stage loading	Secondary loading		Unloading
	Experimental value (mm)	Experimental value (mm)	Theoretical value (mm)	Experimental value (mm)
Mid-span	3.58	4.98	4.63	0.21
A-quarter-span	1.78	2.32	2.41	0
Arch springing	-0.15	-0.50	-0.50	0

worse than the theoretical condition, and the local static strength does not meet the requirements. After unloading the test load, the residual strain is less than 20%, indicating that the structure is in an elastic working state. The strain is too large at the J1-3 joint, mainly due to U-shaped cracks at the mid-span. The a-quarter and arch foot of the cross-section meet the requirements, and the structure is in elastic work. The upper structure of the bridge is a truss arch. Before the test, several transverse cracks were found at the bottom of the middle span. During the test, the strain data gradually increased, and there was no sudden increase, indicating that no new cracks were found.

3.5. Dynamic Load Test. The pulsating method was used to excite the vibration of the bridge structure for the dynamic load test and then determine its natural frequency, damping ratio, vibration mode, etc. Sensors were installed on the bridge and collected signals synchronously. Various disturbances in the environment are regarded as input signals; the signal collected by the sensor is regarded as the output signal of the bridge. The collected time domain signal was transformed into a frequency domain signal by a fast Fourier transform (FFT), and the peak value of the frequency domain signal curve corresponds to the natural frequency of the bridge. In this test, the measuring points were arranged

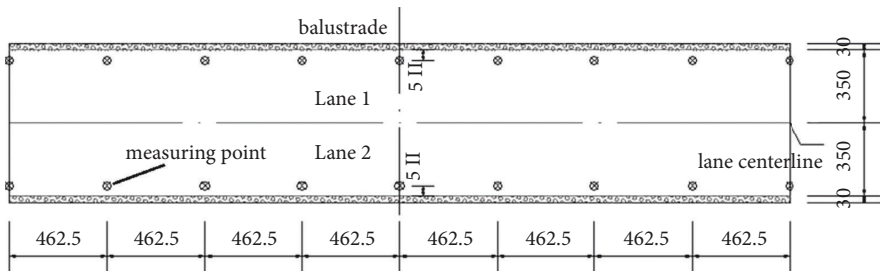

Figure 10: Measuring point arrangement.

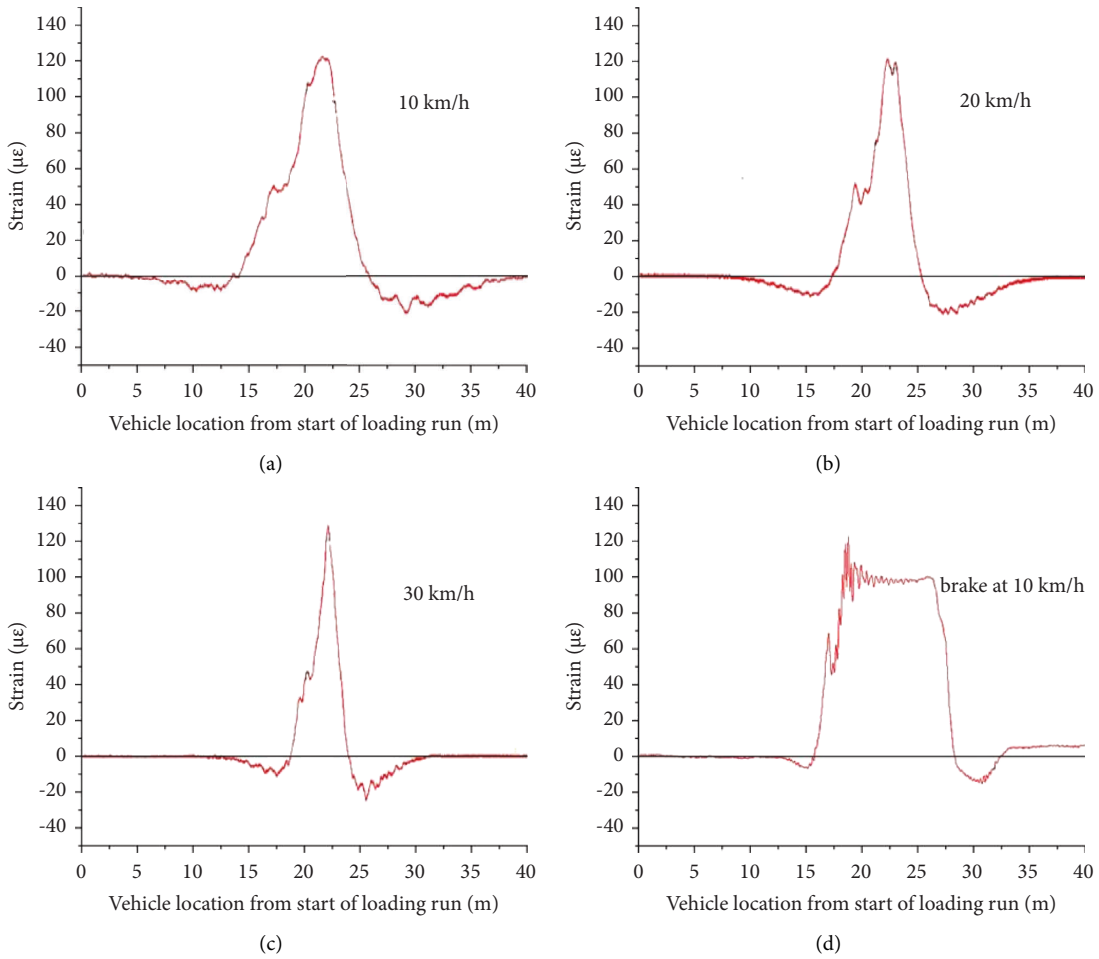

Figure 11: Experimental strain value at middle span. (a) 10 km/h. (b) 20 km/h. (c) 30 km/h. (d) Brake at 10 km/h.

Table 3: Modal parameters.

Vibration mode	Frequency (Hz)	Description of vibration mode
1	6.194	First-order vertical bending vibration
2	9.613	First-order lateral bending-torsional coupled vibration

in eight different locations, and the measuring points were arranged on both sides of the bridge in the transverse direction. Each test point is numbered as points 1~9, keeping the same straight line as illustrated in Figure 10.

Three different speed conditions were selected, 10 km/s, 20 km/s, and 30 km/s, and a brake experiment was completed when a vehicle reached the test position at a constant speed of 10 km/h to implement an emergency brake to generate greater braking force and form a certain impact. The strain value at the middle span of the bridge in the dynamic load test is shown in Figure 11. The frequency of the bridge can be measured, as shown in Table 3.

Table 4: Impact factor at different speeds at middle span.

Machine speed	Position	Impact factor
10 km/h	Mid-span	0.193
20 km/h	Mid-span	0.233
30 km/h	Mid-span	0.261
Brake at 10 km/h	Mid-span	0.213

Table 5: Model parameters.

Parameter	Symbol	Value
Spring constant of suspension	k_{11}	1577000 N/m
	k_{21}	4724000 N/m
Damping of suspension	C_{11}	11200 N/(m/s)
	C_{21}	33420 N/(m/s)
Spring constant of tire	k_{11}	3146000 N/m
	k_{21}	4724000 N/m
	k_{31}	4724000 N/m
Damping of tire	C_{11}	13300 N/(m/s)
	C_{21}	10000 N/(m/s)
	C_{31}	10000 N/(m/s)
Vehicle mass	M	33000 kg
	m_1	700 kg
	m_2	1300 kg
Vehicle geometry	λ_x	5.4 m
	λ_{x1}	4 m
	λ_{x2}	1.4 m
	λ_y	1.8 m
	λ_{y1}	0.9 m
	λ_{y2}	0.9 m
	λ_{y3}	0.6 m

According to the bridge width and section form, the relevant formulas of truss-arch bridges were searched from the General Specifications for Design of Highway Bridges and Culverts (JTG D60-2015). The Chinese code is based on the fundamental frequency of the bridge and the empirical formula, which is a safety-oriented design. The formulas for the impact factor are as follows [1]:

When $f < 1.5\,Hz$, $\mu = 0.05$,

When $1.5\,Hz \le f \le 14\,Hz$, $\mu = 0.1767\mathrm{In}f - 0.0157$,

When $f > 14\,Hz$, $\mu = 0.45$, where f is the fundamental frequency of the structure and μ is the impact factor in the formula. The impact factor based on the fundamental frequency of the bridge can be calculated (the maximum allowable value of the impact factor in the specification):

$\mu = 0.1767\mathrm{Inf} - 0.0157 = 0.307$ (theoretical: 0.261).

The impact factor can also be calculated by definition and the calculation expression is

$$\mu = \frac{Y_{d\max}}{Y_{j\max}} - 1, \tag{2}$$

where $Y_{d\max}$ is the maximum dynamic strain or deflection of the observation point in the dynamic load test; $Y_{j\max}$ is the maximum static strain or deflection of the observation point in the static load test. The results are shown in Table 4. The impact factor of the bridge is increased after the vehicles speed up. Bridge vibration is easier when the vehicle excitation frequency is close to the bridge frequency [25].

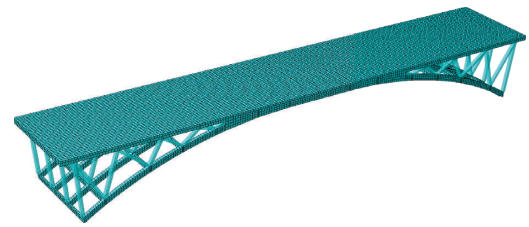

Figure 12: Finite element model of the bridge.

4. Finite Element Analysis

4.1. Bridge Finite Element Model. We collected the dimensions of the bridge components in the field and adjusted the model according to the field collected data. The bridge model was built in the large finite element software ABAQUS and contained a total of 12346 elements and 21832 nodes. The mesh size was 0.2×0.2 m. Each component of the bridge was established according to the measured data. The density and Young's modulus of reinforced concrete were 2549 kg/m^3 and 3.45×10^{10} Pa, respectively, and the others are shown in Table 5. The properties' values were reduced accordingly for the damaged components. The arch and diaphragm beam were modelled by the solid element C3D8R, the bridge deck was modelled by the shell element, and the beam was modelled by the B31 beam element, as illustrated in Figure 12.

4.2. Mode Shape in Finite Element Model. Mode shape is the inherent vibration characteristic of a structural system. Higher order modes contribute less to bridge vibration, and the modal synthesis method can reduce operation time effectively. Modal dynamic analysis in ABAQUS was chosen, and superposition of the first six modes was used in this bridge [26, 27]. The first mode had the greatest influence on the bridge, and higher modes had little effect on the bridge structure. When the bridge frequency is close to the vehicle excitation frequency, the bridge vibrates easily; the first six modes are shown in Figure 13. Table 6 is an introduction to the finite element model data.

4.3. Fundamental Assumption. The vehicle model assumes the following three points: (1) the mass of the tire can be neglected since it is small when compared to the total mass of the vehicle (2) tires close to the ground, even with the effect of road surface roughness (3) the height of the tires and suspensions is the same when the ground is flat and the vehicle is still.

The following conditions should be satisfied in numerical analysis: (1) vehicles travel through bridge structures at a constant speed. (2) The bridge is stationary initially. (3) Vehicles are driven in the prescribed lanes.

4.4. Road Surface Roughness. The model of the bridge deck is difficult to be established in the finite element method, especially if the bridge deck is damaged. The road surface

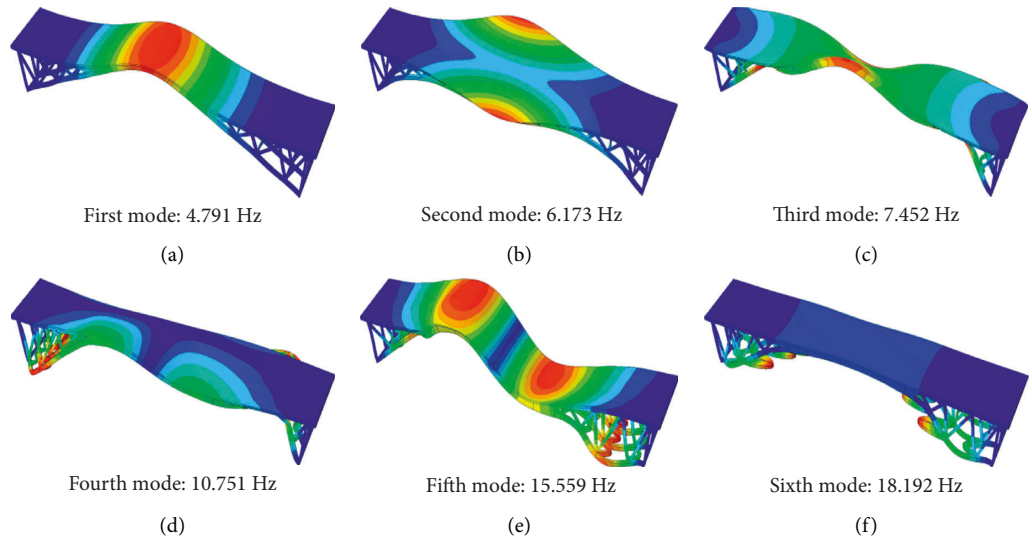

Figure 13: First six modes of the truss-arch bridge. (a) First mode. (b) Second mode. (c) Third mode. (d) Forth mode. (e) Fifth mode. (f) Sixth mode.

Table 6: Bridge properties.

Properties	Size (m)	Moment of inertia (cm^4)
Horizontal linkages beam	0.14×0.55 (rectangle)	1.941×10^5
Truss beam	0.27×0.25 (rectangle)	3.516×10^4
Damping constant	0.02	
Fundamental frequency (model, Hz)	First mode (bending)	4.791
	Second mode (torsion)	6.173

Table 7: Roughness coefficient for different surface conditions.

Condition	Roughness coefficient $a(10^{-6})$	Condition
"Very good"	0~2	"Very good"
"Good"	2~8	"Good"
"Average"	8~32	"Average"
"Poor"	32~128	"Poor"

roughness needs to be simulated to reflect the damage to the bridge deck in MATLAB. The road surface roughness is one of the main factors and is distributed in a random fashion continuously, which affects the dynamic behavior of both the vehicle and the bridge. According to the road level, the random road surface roughness model under certain circumstances can usually be generated by an inverse Fourier transform based on the corresponding power spectral density function, and the power spectrum describes the mean square amplitude of road geometry deviation as a function of the spatial frequency of the irregularities. When programmed as a stationary Gaussian random process, the road surface roughness can be represented as [28]

$$r(x) = \sum_{k=1}^{N} \sqrt{2G_d(n_k)\Delta n} \cos\left(2\pi n_k + r\theta_k\right), \quad (3)$$

where $G_d(n_k) = a/(2\pi n_k)^2$ is the power spectrum analysis (PSD) function in MATLAB and a is the roughness coefficient, which represents different coefficients according to

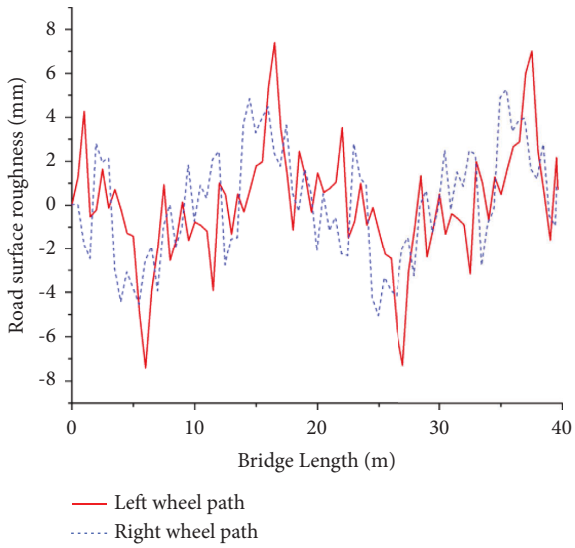

Figure 14: Road surface roughness for left and right wheel paths.

the road conditions. The International Standard Organisation (ISO) divides road surface roughness into four conditions: A-D (from good to poor), and the value of a is illustrated in Table 7. Through our investigation, coefficient "a" is chosen as 8×10^{-6}, which corresponds to an average surface condition. Δn is the frequency interval; $\Delta n = n_{\max} - n_{\min}/N$ here $n_{\max} dn_{\min}$ presents the upper and

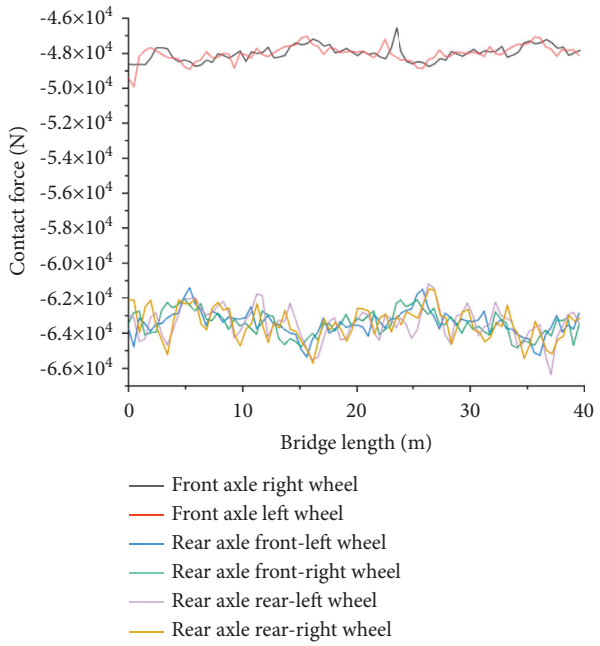

Figure 15: Contact forces at six vehicle axles.

lower cut-off frequencies, respectively; n_k represents the frequency of each wave, where $n_k = n_{\min} + (k-1)\Delta n$ coefficient "N" represents the wave number; and θ_k is the random phase angle uniformly distributed from 0 to 2π. The road surface roughness is calculated by Kim, and the road surface roughnesses of the left and right wheel paths resemble each other, as illustrated in Figure 14.

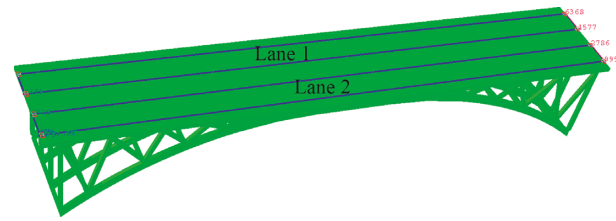

Figure 16: Lane path.

4.5. Contact Point. The tires of vehicles and bridges always change at all times. The tires will cause the subsidence of the bridge and also affect itself during the movement. When a vehicle tire contacts the road surface, the vehicle tire deforms and contacts the road to form a rectangular contact surface. This is called multipoint contact [28]. When the road surface roughness is poor, this model can improve the calculation accuracy of the tire friction. By treating the contact condition between the tire and the road surface as a point contact, one point may overestimate the dynamic deflection of the bridge, and the design is conservative.

When vehicles cross the bridge, road surface roughness will affect the property of the vehicle, which means that tires are close to the ground while eight degrees of freedom of the vehicle model change uninterruptedly [29]. Therefore, we imported the data into the vehicle model and established the corresponding model in MATLAB. The specific method can be seen in Dr. LU's graduation thesis [30], using a differential equation to calculate the subprogram SIMULINK. Due to the length of the article, this article does not give too much explanation.

The motion equation of the vehicle can be derived from the Lagrange equation:

$$\begin{aligned} [M_v]\{\ddot{u}\} + [C_v]\{\dot{u}\} + [K_v]\{u\} &= \{F_g\} + \{F_c\}, \\ \{F_b\} = [K_C]^T\left([K_v]\{F_g\}\right)\%\setminus[C_c]^T\{\dot{u}\} + [K_c]^T\{u\} + [K_r]\{Z_w\} + [C_r]\{\dot{Z}_w\}. \end{aligned} \tag{4}$$

The motion equation of the vehicle can be derived from the Lagrange equation:M_v, C_v, and K_v are the mass, damping, and stiffness matrices of the vehicle, respectively; Kr and Cr are the tire stiffness and damping matrices, respectively. $\ddot{u}$, $\dot{u}$, and u are acceleration, velocity and displacement vectors of vehicle motion; F_g is the gravity vector; F_c is the vector of force and moment applied to the vehicle by the bridge; and f_b is the load unit acting on the bridge. The position of the vehicle is always changing during driving. The dynamic characteristics of the vehicle-bridge coupling system are represented by a block submatrix. Road surface roughness was imported into the vehicle model. The bridge deck contact force calculation is shown in Figure 15.

4.6. Vehicle Driving Process. Modal dynamic analysis is selected in ABAQUS, and the analysis process is divided into three parts: (1) vehicles enter the bridge, (2) vehicle through the bridge, and (3) vehicles pass the bridge, and the bridge is free vibrated. The process was investigated by modal superposition through the previous six modes of the bridge model. The Zhihong Bridge is a two-lane bridge with 204 units in each lane. Heavy vehicles enter from the left side of

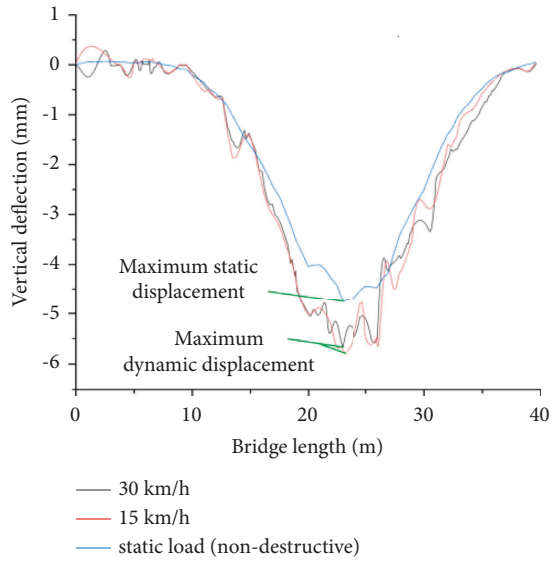

Figure 17: The bridge deflection curve.

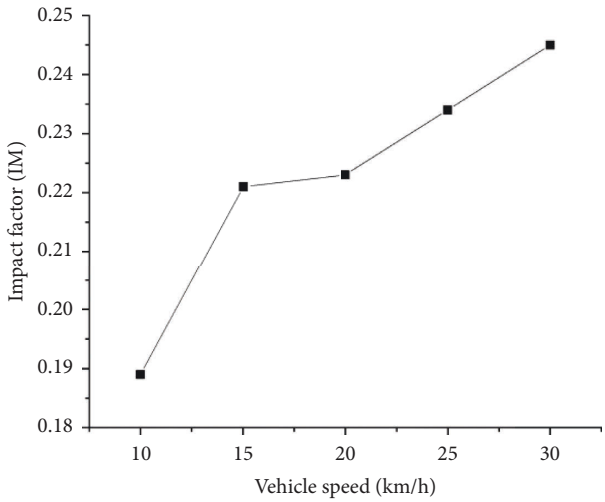

Figure 18: The impact factor at mid-span.

the bridge together, and vehicles are located in the middle of the lane to test the maximum strain and deflection of the bridge, as illustrated in Figure 16.

4.7. Results for Finite Element Method. The contact force applied on the bridge deck in ABAQUS was used to simulate various different working conditions through the general solver. For the process of the vehicle crossing a bridge, the displacement and contact force between the bridge deck and the wheel need to be balanced through the contact point, the bridge model can be discretized by the finite element method through the commonly used the Newmark-β method. The equation at each discrete time is obtained by direct numerical integration calculation. Time is used as a parameter for iteration, and the matrix form is used to ensure the convergence of bridge displacement within each time step.

The impact factor can be expressed by the ratio of the deflection under moving vehicle loading and the deflection under static loading (the formula is usually used in numerical simulation), and the mid-span deflection is the largest in the finite element model. The expression of the impact factor is [31]

$$IM = \frac{(\delta_d - \delta_s)}{\delta_s} \times 100\%, \tag{5}$$

contact $\delta_d$is the maximum dynamic vertical deflection, and $\delta_s$is the maximum static vertical deflection.

Five working conditions were simulated at different speeds (10 km/s, 15 km/s, 20 km/s, 25 km/s, and 30 km/s). Because it is a small- and medium-span concrete bridge, the speed cannot be too fast. There is little difference in bridge deflection at different speeds, taking 15 km/h and 30 km/h as examples to compare nondestructive bridges, as illustrated in Figure 17. It shows that the damage has a great influence on bridge vibration under heavy vehicles. The impact factor (IM) at mid-span of the bridge is illustrated in Figure 18.

The truss-arch bridge is the most disadvantaged structure in mid-span. The measured bridge is more seriously damaged than the finite element simulation bridge under the action of long-term heavy load. The impact factor obtained at the support and a quarter of the bridge is consistent with the measured data, as illustrated in Figure 19.

The impact factors derived from field load tests are similar to the finite element simulation, and the impact factors are slightly higher than the finite element simulation data with a maximum error of approximately 6%. It is shown that the finite element simulation of the dynamic response of bridges based on vehicle-bridge interaction theory can effectively evaluate the technical status of bridges, and the damage detection of bridges (bridge maintenance) can provide data in real-time for finite element models to ensure the safety of bridges.

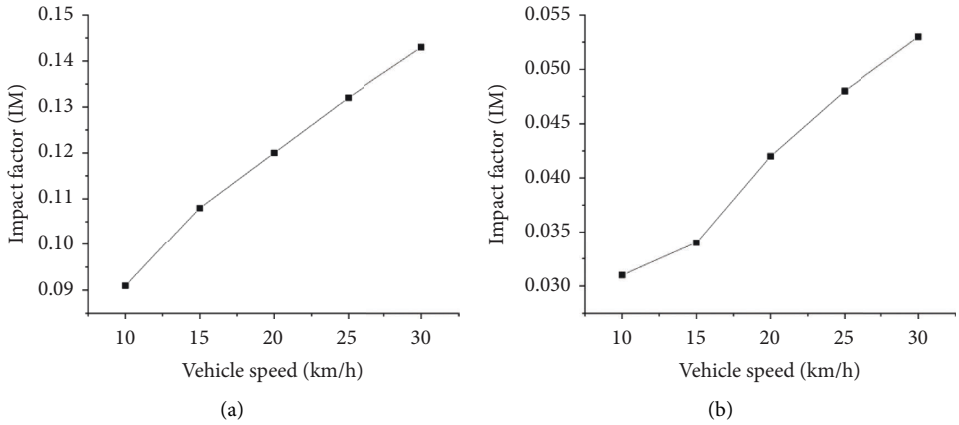

Figure 19: The impact factor in different locations. (a) Support. (b) A quarter of the bridge.

5. Conclusion

(1) Since most countries easily ignore the late management of bridges, and the impact factor to judge whether a bridge is good or bad is mostly based on experience, which makes it difficult to determine the real vibration of the bridge. For the old truss-arch bridge built in the last century, due to concrete cracking, reinforcement corrosion, and bridge cracking occurring, there are the problems of horizontal thrust reduction, uneven forces on the bars, and greater deflection of the arches. Therefore, a fast and safe detection method based on vehicle-bridge interaction theory is proposed. It is necessary to analyze specific problems and adjust parameters according to different bridge structures and vehicle conditions. The parametric analysis of the bridge illustrates that bridge damage can seriously affect the load carrying capacity and the dynamic impact factor IM, this method can be used to assess the service performance of the bridge in various conditions. The impact factors are all lower than the specification through rapid inspection by finite element software and comparative analysis of load tests, and the bridge is in a safe condition for service. The bridge vibrations all occur under elastic deformation, but during heavy vehicle crossings, the bridge deck vibrates at a higher amplitude and the deflection changes of the arches need to be controlled. In order to ensure the safety, serviceability, and durability of the bridge, the bridge defects identified by the finite element simulation results need to be repaired in a timely manner.

(2) According to field inspection, damage to old bridges is generally characterized by multiple cracks in the bottom slab, cracking of the expansion lower diagonal bars, and loosening of concrete by cracking, which will affect the life of the bridge. The structural performance of the bridge deteriorates continuously under the impact of modern traffic flow and heavy vehicles, which will lead to serious structural damage. A vicious cycle will be formed due to the long-term neglect of bridge maintenance, accelerating the destruction of concrete bridges, so bridge damage needs to be detected in time. By this method, the damage to the bridge deck is expressed in FEM by the parameter of road surface roughness, which can effectively reflect the effect of road roughness on bridge vibration and even investigate the jumping problem caused by the damage to the expansion joint filler. The data of the damaged parts of the bridge are imported into the bridge model to analyze the dynamic increase effect of the vehicle on the bridge under various traffic conditions, which can replace the dynamic load test to set up the required test points at the damaged parts and evaluate the technical status of the bridge rapidly at this stage according to the catastrophe values of the dynamic impact factor.

Data Availability

The data used to support the findings of this study are included within the article.

Conflicts of Interest

The authors declare that they have no conflicts of interest.

Acknowledgments

The authors are grateful to the funding support from the National Natural Science Foundation of China (No. 51608343) and Graduate Research Innovation Program (KYCX20_2774).

References

[1] Jtg D60-2004, *General Specifications for Design of Highway Bridges and Culverts*, Ministry of Transport of the People's Republic of China, China, 2004.

[2] B. Bhattacharya, D. Li, M. Chajes, and J. Hastings, "Reliability based load and resistance factor rating using in-

service data," *Journal of Bridge Engineering*, vol. 10, no. 5, pp. 530–543, 2005.

[3] L. Lai, G. S. Baker, and M. S. Dragan, *Load Testing on Two Bridge Superstructures Structures Congress on Engineering Smarter*, pp. 1093–1101, ASCE, New York, NY, USA, 2009.

[4] M. R. DelGrego, M. P. Culmo, and J. T. Dewolf, "Performance evaluation through field testing of century- old railroad truss bridge," *Journal of Bridge Engineering*, vol. 13, no. 2, pp. 132–138, 2008.

[5] S. F. Breña, A. E. Jeffrey, and S. A. Civjan, "Evaluation of a noncomposite steel girder bridge through live-load field testing," *Journal of Bridge Engineering*, vol. 18, no. 7, pp. 690–699, 2013.

[6] T. Terzioglu, D. Jiang, M. B. D. Hueste, J. B. Mander, and G. T. Fry, "Experimental investigation of a full-scale spread slab beam bridge," *Journal of Bridge Engineering*, vol. 21, no. 11, 11 pages, Article ID 040160821, 2016.

[7] I. K. Fang, C.-R. Chen, and I.-S. Chang, "Field static load test on kao-ping-hsi cable-stayed bridge," *Journal of Bridge Engineering*, vol. 9, no. 6, pp. 531–540, 2004.

[8] L. Deng, R. Cao, W. Wang, and X. Yin, "A multi-point tire model for studying bridge-vehicle coupled vibration," *International Journal of Structural Stability and Dynamics*, vol. 16, no. 08, Article ID 1550047, 2016.

[9] L. Deng and F. Wang, "Impact factors of simply supported prestressed concrete girder bridges due to vehicle braking," *Journal of Bridge Engineering*, vol. 20, no. 11, Article ID 06015002, 2015.

[10] L. Deng, W. He, and Y. Shao, "Dynamic impact factors for shear and bending moment of simply supported and continuous concrete girder bridges," *Journal of Bridge Engineering*, vol. 20, no. 11, Article ID 04015005, 2015.

[11] N. Zhang, Z. Zhou, and Z. Wu, "Safety evaluation of a vehicle–bridge interaction system using the pseudo-excitation method," *Railway Engineering Science*, vol. 30, no. 1, pp. 41–56, 2022.

[12] E. Chen and X. Zhang, "Dynamic analysis of viscoelastic asphalt pavement under vehicle–bridge interaction load," *Journal of Transportation Engineering, Part B:Pavements*, vol. 147, 4 pages, 2021.

[13] L. Zhang, D. Feng, and G. Wu, "Simultaneous identification of bridge damage and vehicle parameters based on bridge strain responses," *Structural Control and Health Monitoring*, vol. 29, no. 6, Article ID e2945, 2022.

[14] Y. Luo, H. Zheng, H. Zhang, and Y. Liu, "Fatigue reliability evaluation of aging prestressed concrete bridge accounting for stochastic traffic loading and resistance degradation," *Advances in Structural Engineering*, vol. 24, no. 13, pp. 3021–3029, 2021.

[15] T. L. Wang, D. Z. Huang, and M. Shahawy, "Dynamic response of multigirder bridges," *Journal of Structural Engineering*, vol. 118, no. 8, pp. 2222–2238, 1992.

[16] N. K. Harris, E. J. Obrien, and A. González, "Reduction of bridge dynamic amplification through adjustment of vehicle suspension damping," *Journal of Sound and Vibration*, vol. 302, no. 3, pp. 471–485, 2007.

[17] D. Huang and T. L. Wang, "Impact analysis of cable stayed bridges," *Computers & Structures*, vol. 43, no. 5, pp. 897–908, 1992.

[18] L. Deng, W. He, and Yuy, "Research progress in theory and applications of Highway vehicle-bridge coupling vibration," *China Journal of Highway and Transport*, vol. 31, no. 7, pp. 38–54, 2018.

[19] Z. Sun and Z. Zou, "Towards an efficient method of predicting vehicle-induced response of bridge," *Engineering Computations*, vol. 33, no. 7, pp. 2067–2089, 2016.

[20] M. Sokol, M. Venglár, K. Lamperová, and M. Marfoldi, "Performance assessment of a renovated precast concrete bridge using static and dynamic tests," *Applied Sciences*, vol. 10, no. 17, 5904 pages, 2020.

[21] I. B. L. U. Zhang, S. Wang, and L. I. Bing, "Dynamic response of a vehicle-bridge expansion joint coupled system," *Shock and Vibration*, vol. 2016, Article ID 1621589, , 2016.

[22] X. Q. Zhu and S. S. Law, "Dynamic load on continuous multilane bridge deck from moving Vehicles," *Journal of Sound and Vibration*, vol. 251, no. 4, pp. 697–716, 2002.

[23] C. W. Kim, M. Kawatani, and K. B. Kim, "Three-dimensional dynamic analysis for bridge vehicle interaction with roadway roughness," *Computers & Structures*, vol. 83, no. 19-20, pp. 1627–1645, 2005.

[24] Jtg/T J21-01-2015, *Load Test Methods for Highway Bridge*, Ministry of Transport of the People's Republic of China, China, 2016.

[25] H. Li, *Dynamic Response of Highway Bridges Subjected to Heavy Vehicle*, Florida State University, Tallahassee, 2005.

[26] C. S. Cai, X. M. Shi, M. Araujo, and S. Chen, "Effect of approach span condition on vehicle-induced dynamic response of slab-on-girder road bridges," *Engineering Structures*, vol. 29, no. 12, pp. 3210–3226, 2007.

[27] J. C. Wyss, D. Su, and Y. Fujino, "Prediction of vehicle-induced local responses and application to a skewed girder bridge," *Engineering Structures*, vol. 33, no. 4, pp. 1088–1097, 2011.

[28] C. J. Dodds and J. D. Robson, "The description of road surface roughness," *Journal of Sound and Vibration*, vol. 31, no. 2, pp. 175–183, 1973.

[29] L. Deng and C. S. Cai, "Development of dynamic impact factor for performance evaluation of existing multi-girder concrete bridges," *Engineering Structures*, vol. 32, no. 1, pp. 21–31, 2010.

[30] S. B. Lu, *Study on Vehicle Chassis Key Subsystems and its Integrated Control Strategy*, Chongqing University, Chongqing, 2009.

[31] L. Deng, Y. X. Chen, and W. S. Han, "Studying impact factors for short and medium span simply supported concrete Highway bridges and its suggested values," *China Journal of Highway and Transport*, vol. 33, no. 1, pp. 69–78, 2020.